11-15-1987

The Onset of Spring Melt in First-Year Ice Regions of the Arctic as Determined From Scanning Multichannel Microwave Radiometer Data for 1979 and 1980

Mark R. Anderson
University of Nebraska-Lincoln, manderson4@unl.edu

JOURNAL OF GEOPHYSICAL RESEARCH, VOL. 92, NO. C12, PAGES 13,153–13,163, NOVEMBER 15, 1987

The Onset of Spring Melt in First-Year Ice Regions of the Arctic as Determined From Scanning Multichannel Microwave Radiometer Data for 1979 and 1980

MARK R. ANDERSON[1]

Climate and Remote Sensing Group, Scripps Institution of Oceanography, University of California, San Diego, La Jolla

Sea ice ablation is an important physical process affecting the global climate system. During the Arctic melt season, rapid changes occur in both sea ice surface conditions and the extent of ice. These changes alter the albedo and vary the surface energy budget. Understanding variations in Arctic sea ice is critical for global climate studies. This paper investigates the spring onset of melt in the Arctic seasonal sea ice zone through analysis of melt signatures derived from Nimbus 7 scanning multichannel microwave radiometer data. Satellite-derived melt signatures, determined by 18- and 37-GHz vertical brightness temperatures, are associated with the initial melt of the snow pack on the sea ice surface. Sea ice melt events vary spatially and temporally. Within the arctic basin the melt signature is observed first in the Chukchi Sea and the Kara and Barents seas. As melting progresses, the melt signature moves westward from the Chukchi Sea and eastward from the Kara and Barents seas to the Laptev Sea region. The initial location of the melt signal also varies with year. In 1979 the melt signature occurs first in the Chukchi Sea; and in 1980 in the Kara Sea. The date for the initial melt varies between 1979 and 1980 by an average of 7–10 days with a maximum of 25 days in the Chukchi Sea region. Monitoring the occurrence of melt signatures can be used as an indicator of climate variability in the Arctic's seasonal sea ice zones.

1. INTRODUCTION

Sea ice plays an integral role in the global climate system, affecting climate through changes in surface albedo, sensible and latent heat exchanges, and salinity profiles of the underlying ocean. These variations in sea ice are particularly significant during the melt season, when rapid changes in ice extent and surface conditions occur.

Originally, the spatial distribution of melt in the Arctic was believed to occur latitudinally around the North Pole as the result of increasing solar radiation during the melt season [*Marshunova and Chernigovskiy*, 1978]. Point observations from drifting Soviet ice stations, however, suggest that the melt pattern is more involved than was first thought [*Chukanin*, 1954; *Yanes*, 1966]. Aircraft measurements further illustrate the complex nature of spring melt patterns [*Kuznetsov and Timerev*, 1973]. The primary problem for studying the Arctic melt patterns is the scarcity of data, especially for surface conditions during melt of the ice and snow cover.

Passive microwave remote sensing, with its nearly all-weather, all-season capabilities, has increased our understanding of the spatial distribution of Arctic melt. *Campbell et al.* [1984], using the single channel Nimbus 5 electrically scanning microwave radiometer (ESMR) data, describe the spatial progression of melt across the Arctic. *Carsey* [1984, 1985], on the other hand, presents temporal variations of the ESMR data during spring and summer for multiyear ice regions. Passive microwave response to different ice melt conditions is further investigated by recent field work, both on the ice [*Grenfell and Lohanick*, 1985] and in outdoor laboratory conditions [*Grenfell*, 1985; *Gow*, 1985]. Additional work by *Anderson et al.* [1985], using Nimbus 7 scanning multichannel microwave radiometer (SMMR) derived data, illustrates regions of spurious multiyear ice signatures in first-year ice regions of the Kara and Barents seas during spring 1979. They conclude that these spurious signatures are a result of emissivity changes brought about by snow melt on the sea ice surface. This paper uses the hypothesis developed by *Anderson et al.* [1985] for the Kara and Barents seas and applies it to other regions in the Arctic seasonal sea ice zone (Figure 1) to illustrate the timing and spatial variability of the spring melt.

2. MICROWAVE DATA

The Nimbus 7 SMMR, launched in October 1978 and still operational, records passive microwave radiation in both horizontal and vertical polarizations for five frequencies (wavelengths): 6.6 GHz (4.6 cm), 10.7 GHz (2.8 cm), 18 GHz (1.7 cm), 21 GHz (1.4 cm), and 37 GHz (0.81 cm). The Nimbus 7 platform has a near-polar orbit at an altitude of 955 km and a swath width of 780 km [*Gloersen and Hardis*, 1978]. Because of power limitations on the Nimbus-7 platform, SMMR operates only on alternate days.

The SMMR data used in this study are collected from two archive tape formats: CELL-ALL and MAP-SS. (For a complete description of all the SMMR data, refer to either *Gloersen et al.* [1984] or the SMMR data handbook [*NASA*, 1984]). CELL-ALL orbital data tapes, for April 1 to July 31, 1979 and 1980, provide 60-km-resolution 18-GHz and 37-GHz brightness temperatures. Appling the same methodology used to produce the MAP-SS data, the brightness temperatures are binned into a 60-km grid. These data are binned for each data day, and then every 2 data days, an interval of 4 calendar days is averaged. Gridded sea ice concentrations and multiyear ice fractions are collected from the MAP-SS data tapes. The MAP-SS data also consist of 4-calendar-day averages. The methods for retrieving the

[1] Now at Climatology Program, Department of Geography, University of Nebraska, Lincoln.

Paper number 7C0637.
0148-0227/87/007C-0637$05.00

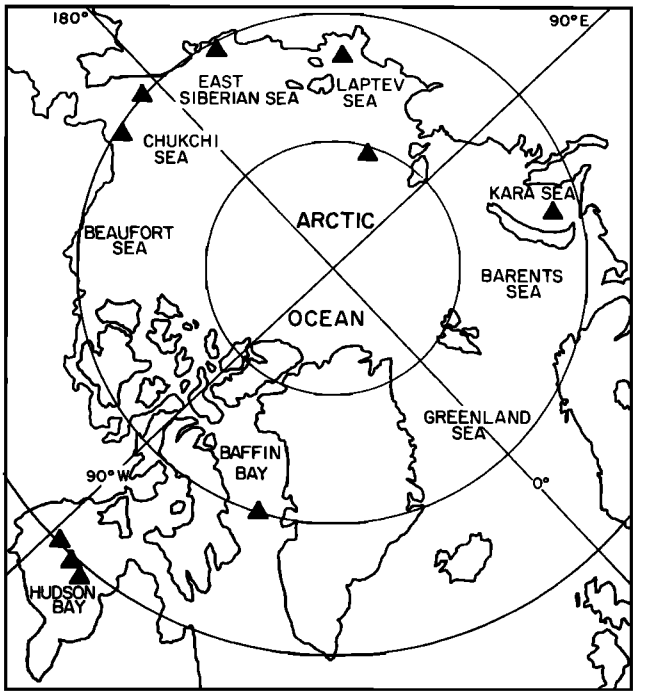

Fig. 1. The arctic region, with study locations represented by triangles.

SMMR sea ice parameters used in this study are described by *Cavalieri et al.* [1984].

3. SMMR Melt Signature

Using multiyear ice fractions derived from SMMR data, *Anderson et al.* [1985] show that while the multiyear sea ice fractions appear realistic during the winter months, spurious indications of multiyear ice are observed in first-year ice regions of the Kara and Barents seas during spring 1979. They conclude that these areas are a result of changes in surface emissivity during spring melt. Spurious regions of multiyear ice are also observed in other sections of the Arctic seasonal sea ice zone for 1979 and 1980. To explain these occurrences more fully, a detailed examination of possible causes is conducted for each location. Since ground truth data are not available, analogies are drawn from recent work, including both satellite interpretations as well as previous field work. For the purpose of this paper, the possible explanations for the spurious multiyear ice fractions are presented below in a general overview, rather than on a regional basis.

Ice remaining in a region through the previous summer melt could produce a multiyear ice signature. Analysis of sea ice charts reveals that in the majority of cases ice did not last through the summer. When it did, concentrations were small, and there was no indication of the multiyear ice by passive microwave measurements in the fall or winter. For example, in the southwest portion of the Kara Sea for the years 1979 and 1980, ice remained along the Novaya Zemlya coast through the summer melt. However, the area covered by sea ice is small, and the concentrations reported on the Navy–National Oceanic and Atmospheric Administration (NOAA) Joint Ice Center (JIC) sea ice charts are low, 20 to 40%. The British Meterological Office monthly sea ice charts for 1962–1983 also show that the 2 years 1979 and 1980 are the only periods during which ice is reported to have lasted the summer melt. It should be noted that the Navy-NOAA JIC sea ice charts incorporate SMMR data in their analysis; the British Meterological Office, however, does not. In addition, no ice is reported in the adjacent Barents Sea, and the multiyear ice signature is still present during the spring. Moreover, multiyear ice signatures are not observed for both locations throughout the year but are observed only at the start of spring melt. In this case and the others presented here, the multiyear ice signatures are not considered to be a result of real ice lasting through a previous summer melt.

There is also the possibility that multiyear ice is advected into a region. This is excluded because of the spontaneous occurrence of the multiyear ice fractions. If advection had taken place, then the multiyear ice could have been traced back to regions where multiyear ice is present. This, however, is not observed; therefore advection can be ruled out.

Atmospheric conditions are also investigated to determine whether the multiyear ice signatures result from liquid precipitation. Examination of Defense Meterological Satellite Program (DMSP) visible imagery shows periods of both clear and cloudy conditions during episodes of spurious multiyear ice signatures. If atmospheric effects are the explanation, then the brightness temperature data would show a more disjunct indication and not a cumulative change as observed. Thus the multiyear ice signatures are probably not due to atmospheric effects.

An additional hypothesis to test is whether the ice goes through a structural change. Variations in brine content are reflected by emissivity changes, and since ice age is a function of brine content, passive microwave data can indicate ice age. It is possible that first-year ice drains its brine and takes on the appearance of older ice. However, time sequences of multiyear ice show that the fractions return to very low values after high spurious values occur. Spatial analysis also shows that advection does not take place after the spurious multiyear ice observations. Therefore the multiyear ice signatures can not be caused by the draining of brine within the ice, since draining is an irreversible process.

It would appear, then, that fluctuations in the multiyear ice fractions are not a consequence of ice advection, ice lasting through the previous summer melt, or atmospheric effects such as precipitation; rather, fluctuations result from surface effects on emissivity other than the draining of brine. To help determine possible mechanisms for emissivity changes, 4-day averaged 18- and 37-GHz brightness temperature time sequences are obtained from the CELL-ALL data tapes and binned to a 60-km grid. For illustrative purposes the binned brightness temperatures for Kara Sea during spring 1979 and 1980 are displayed in Figure 2. Similar patterns are also found for the other studied locations. Multiyear ice fractions plotted in Figure 2 are calculated from the binned brightness temperatures using the SMMR algorithm discussed by *Cavalieri et al.* [1984].

Examination of the brightness temperatures shows a strong decline during the spurious multiyear ice fractions, with a greater decrease in the 37-GHz channel than in the 18-GHz channel. Before the decline there is a slight increase in brightness temperature during April, which should correspond to an increase in liquid water within the snow pack. The decline would then be associated with enlarged crystal sizes and possibly the formation of a crust on the snow

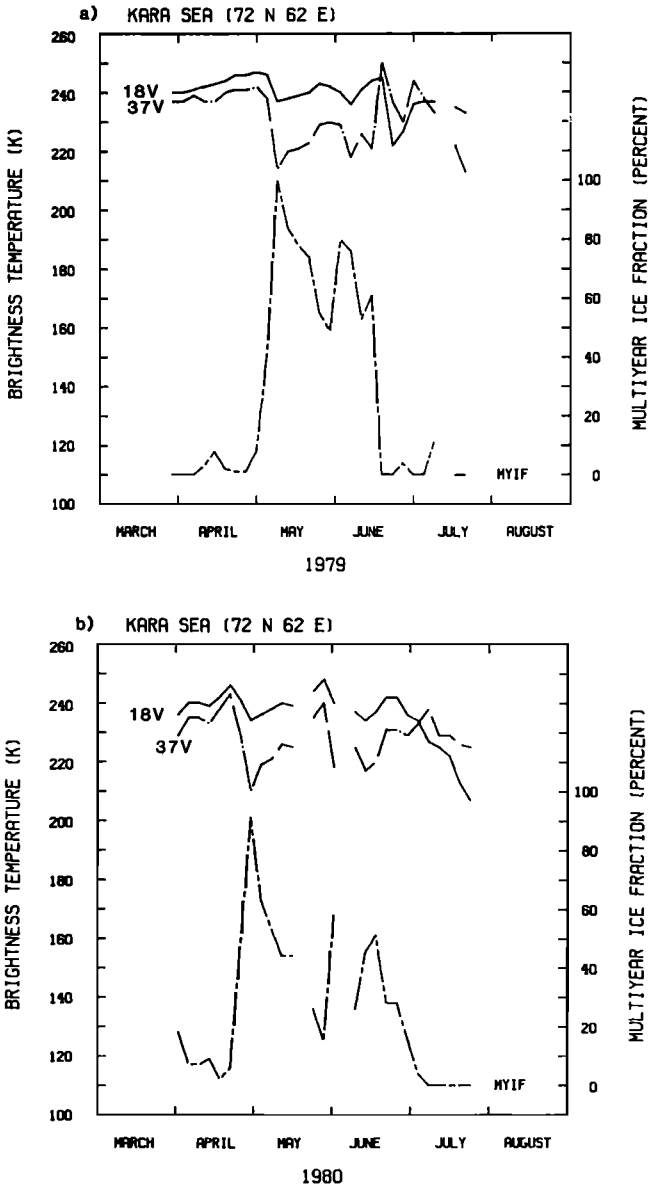

Fig. 2. Time sequence of 18-GHz and 37-GHz brightness temperatures and calculated multiyear ice fractions in the Kara Sea for April through July (*a*) 1979 and (*b*) 1980.

surfaces from melt-freeze cycles [*Gloersen and Campbell*, 1984].

The differential decline in brightness temperature may also be caused by an increase in snow melt to the point where the water content of the snow cover is great enough to lower the emissivity at the higher frequencies [*Comiso et al.*, 1984].

In summary, multiyear ice melt-freeze signatures have been observed using SMMR-derived microwave data for 1979 and 1980 within the seasonal sea ice zones. Examination of these events and the possible physical processes that could cause large multiyear ice fractions suggest that the signatures are due to emissivity changes in the ice surface produced by the onset of spring snow melt. These changes result in the algorithm yielding false indications of multiyear ice.

4. Spring Melt Features

Variations in the physical characteristics and timing of melt across the Arctic seasonal sea ice zone have been recognized from the SMMR data in 1979 and 1980. In general, melt signatures are first observed in the lower latitudes and advance northward with time. Along the Asian Arctic coast, however, melt commences in the far eastern (Chukchi Sea) and western (Barents and Kara seas) sectors and over several weeks progresses zonally toward the central coastal region (Laptev Sea). The timing and duration of melt within a studied region varies by 1 week to several weeks between the 2 years. Monitoring SMMR-derived melt signature occurrences in the seasonal sea ice zone can then be used as an indicator of the onset of melt. The following section gives a more detailed discussion of melt signature occurrences for the locations displayed in Figure 1.

Kara Sea

The seasonal cycle of sea ice in the Kara Sea differs considerably from that at adjacent locations. Freeze-up starts generally by the end of September, with complete ice cover usually occurring by December. By comparison, ice in the Barents Sea does not reach its maximum extent until March or April. This difference is caused by the blockage of warm North Atlantic Drift waters from the Kara Sea by Novaya Zemlya, allowing freeze-up to occur much earlier

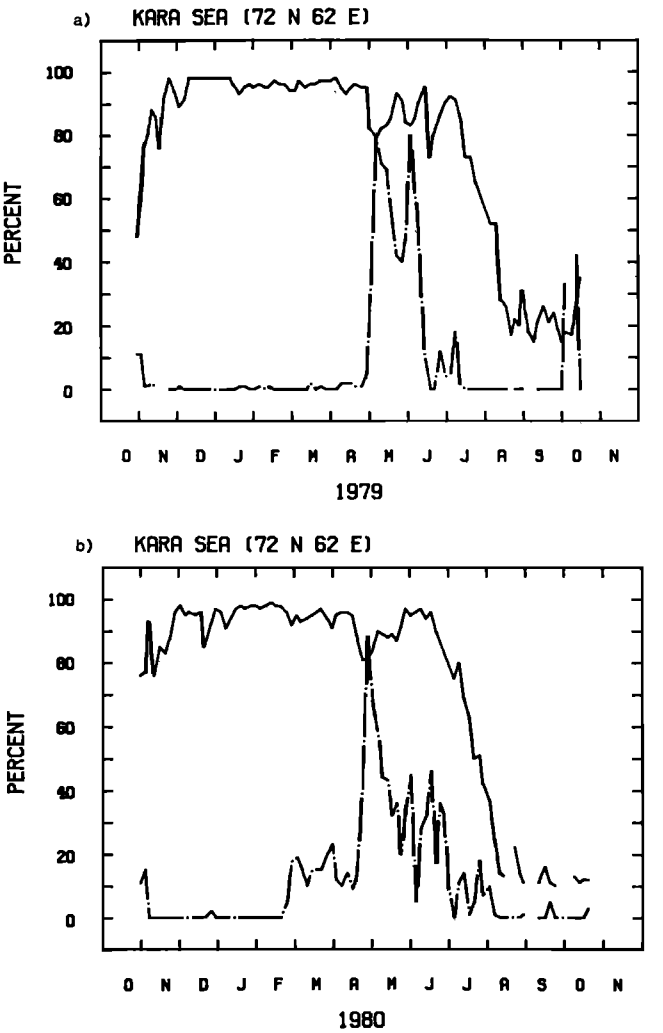

Fig. 3. Time sequence of sea ice concentration (solid line) and multiyear ice fraction (dashed-dotted line) in the Kara Sea for (*a*) October 1978 through October 1979 and (*b*) October 1979 through October 1980.

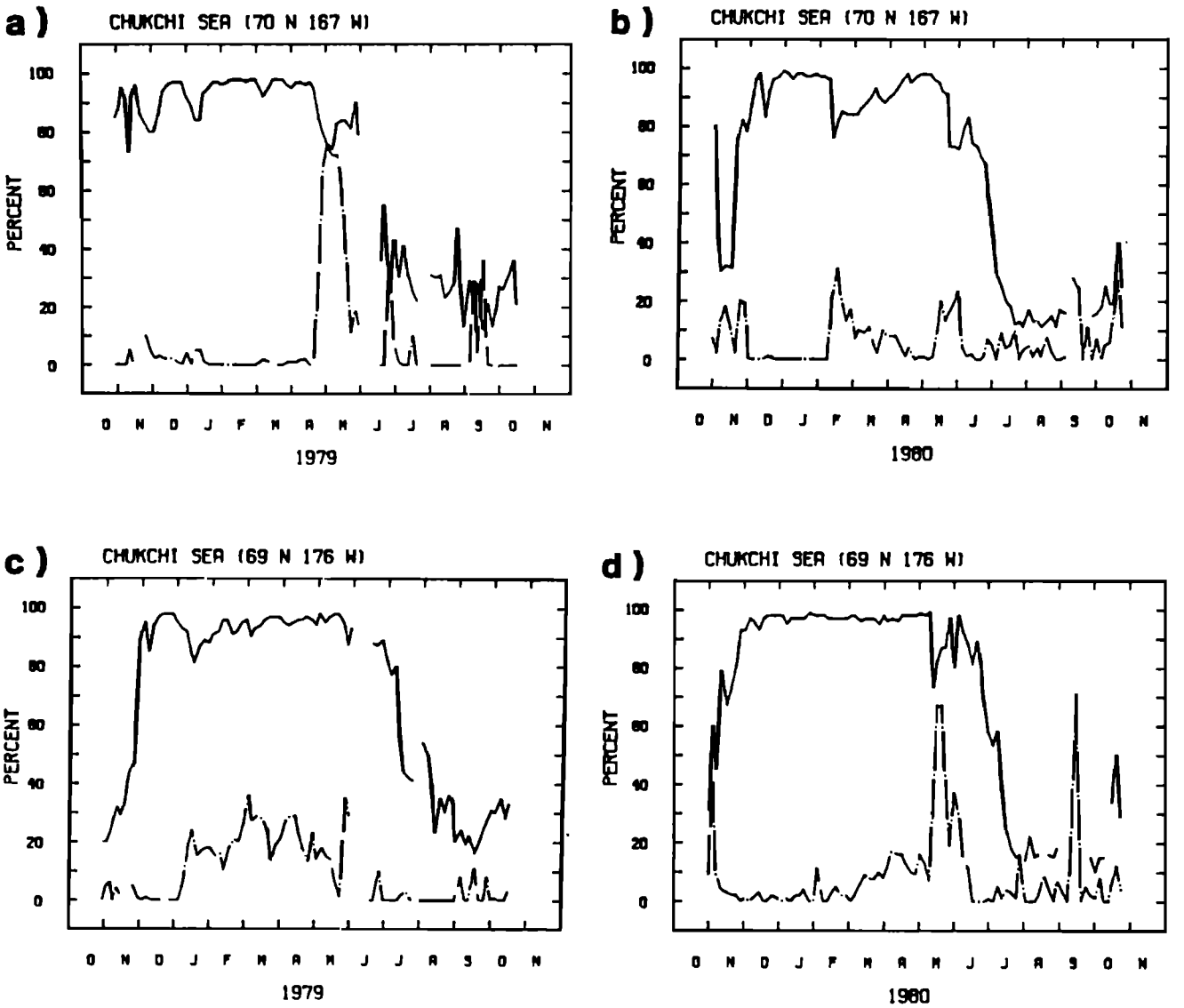

Fig. 4. Time sequence of sea ice concentration (solid line) and multiyear ice fraction (dashed-dotted line) in Chukchi Sea for the Alaskan site during (*a*) October 1978 through October 1979 and (*b*) October 1979 through October 1980 and for the Siberian site during (*c*) October 1978 through October 1979 and (*d*) October 1979 through October 1980.

[*Stringer et al.*, 1984]. Owing to the Kara Sea's landlocked nature, the extent of ice is less variable interannually than that in the Barents Sea, which is controlled by the location and strength of the Icelandic low through its effect on atmospheric advection.

The ice ablation in the Kara Sea also differs from adjacent regions, again mainly because of the region's synoptic weather conditions and geographic location. The first signs of open water occur on average between June 1 and June 15 [*NOAA*, 1984]. These usually form along the coast and are due to flooding of the fast ice from snowmelt runoff from local rivers [cf. *Barry et al.*, 1979]. Sea ice deterioration continues with radiational melting and breakup processes caused by oceanographic and atmospheric conditions. Generally, the southern half of the Kara Sea is completely ice free by the end of the summer.

Time sequences of sea ice concentrations and multiyear ice fractions are produced from SMMR MAP-SS data for the Kara Sea for the spring of 1979 and 1980 (Figure 3). These are computed for a 180 km × 180 km area centered on 72°N, 62°E (Figure 1). The SMMR-derived ice concentration time series display the annual sea ice cycle quite well (Figure 3). In fall 1978, the freeze-up is observed with total ice cover by December. Throughout the winter, small fluctuations of 1–5% occur, due possibly to surface leads in the ice surface, though still within the noise level of the calculations. The sea ice concentration also shows larger changes of 10–20% during the spring melt. These are opposite in direction to the multiyear ice fractions; likewise, the sequence shows the decline in the ice cover until open water is present in August.

Analysis of the multiyear ice fraction time series should show no multiyear ice throughout the year. This, however, is not the case. A rapid increase in the multiyear ice fraction from near zero to 80%, the melt signature, occurs around May 8, 1979. After variations in May and early June, the fraction decreases to zero by the middle of June (Figure 3*a*). It should be noted that the algorithm to determine ice type breaks down after melt, and any subsequent fluctuations should be considered within the noise level [*Cavalieri et al.*, 1984]. The multiyear ice fraction increases observed in

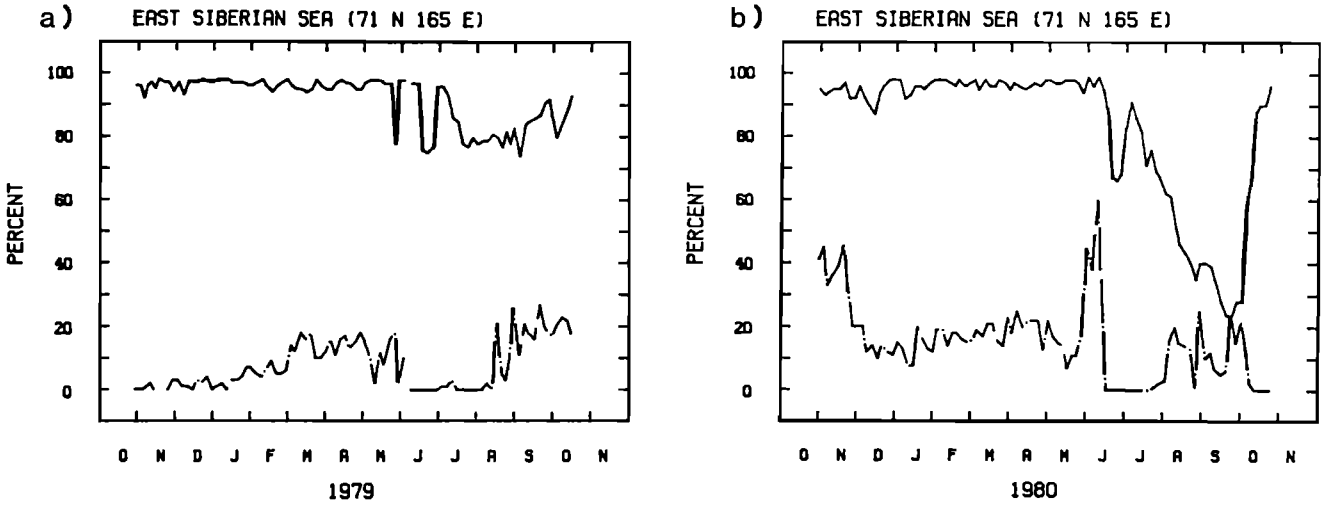

Fig. 5. Time sequence of sea ice concentration (solid line) and multiyear ice fraction (dashed-dotted line) in the East Siberian sea for (*a*) October 1978 through October 1979 and (*b*) October 1979 through October 1980.

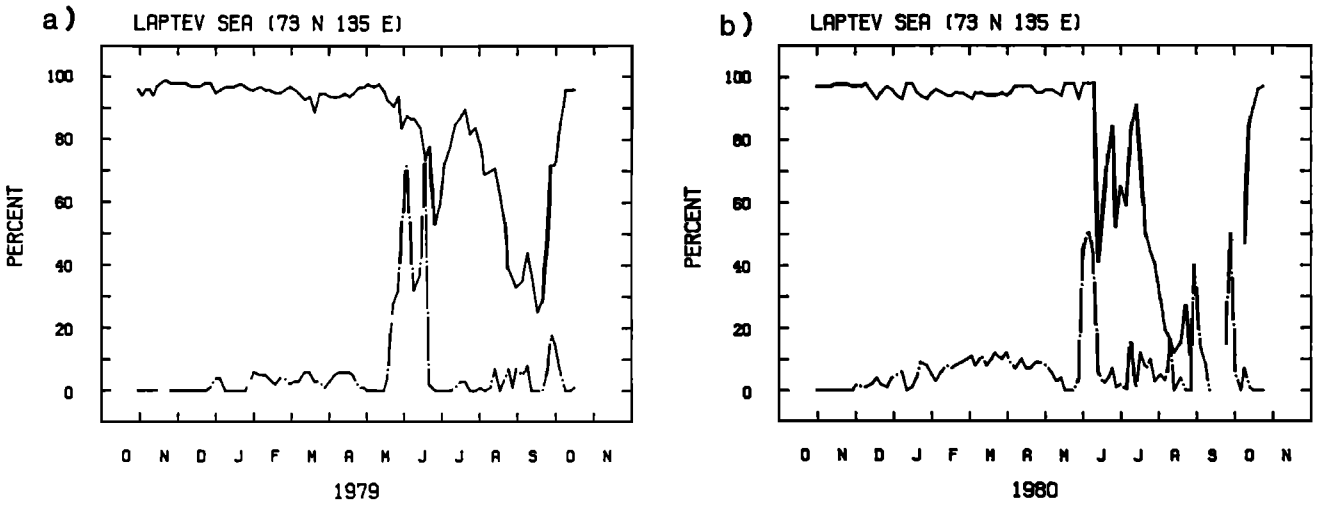

Fig. 6. Time sequence of sea ice concentration (solid line) and multiyear ice fraction (dashed-dotted line) in the southern Laptev Sea for (*a*) October 1978 through October 1979 and (*b*) October 1979 through October 1980.

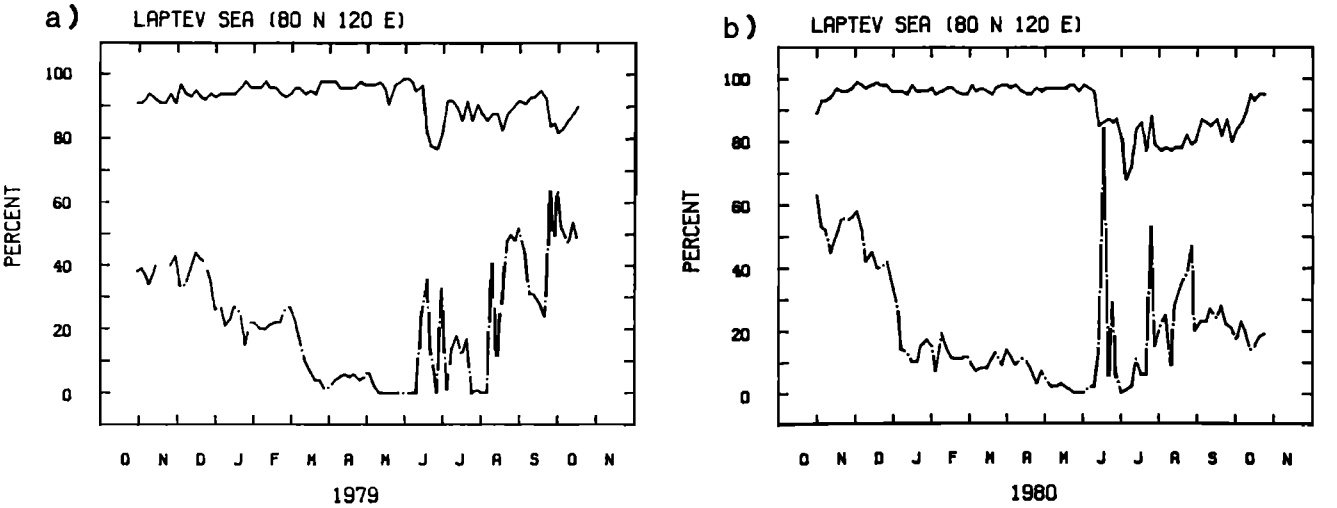

Fig. 7. Time sequence of sea ice concentration (solid line) and multiyear ice fraction (dashed-dotted line) in the northern Laptev Sea for (*a*) October 1978 through October 1979 and (*b*) October 1979 through October 1980.

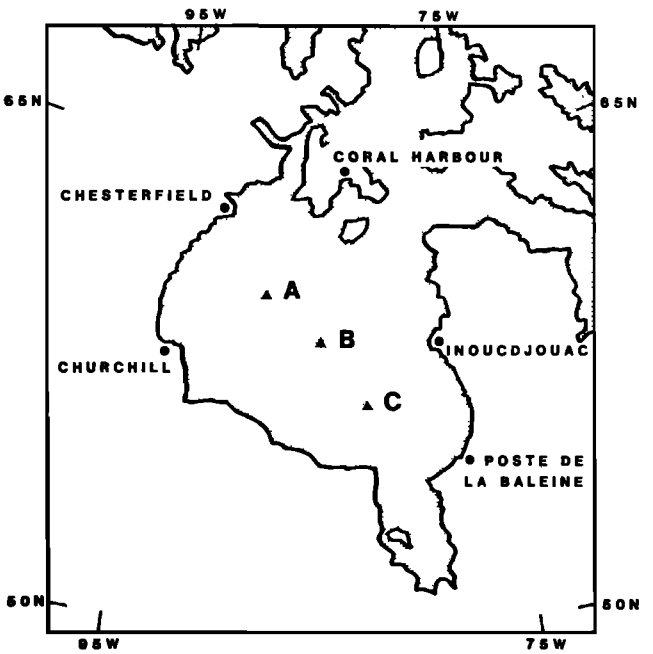

Fig. 8. Hudson Bay region. Study locations are represented by triangles.

October should also be disregarded, since the multiyear ice calculation is not normally computed when the ice concentration is less than 30% [*Cavalieri et al.*, 1984]. These erroneous fractions are probably the result of the time and space averaging techniques used in this study.

The time sequences of sea ice concentration and multiyear ice fraction for 1980 (Figure 3*b*) show the melt signature occurring in late April. The small variations that take place from the beginning of March until the large increase in April can again be considered within the noise level of the microwave data. The occurrence of the melt signature is also 10–12 days earlier than that in 1979. In addition, it drops off later in 1980, near the end of June, 2 weeks later than in 1979.

Chukchi Sea

In the Chukchi Sea (Figure 1), differences in the timing of the melt signatures are again found between 1979 and 1980. In 1979 the signature is first observed during mid-April in the Chukchi Sea off Alaska (Figure 4*a*), while the Siberian location (Figure 4*c*) shows no apparent signature during the month of April. A melt signature for the Siberian site appears to begin at the end of May. However, there were no data archived in the MAP-SS format during this period. Even if the data were to show a melt signature, it would be a month later than that observed at the Alaskan site.

In general, sea ice breakup in the Chukchi Sea occurs first along the Alaskan coast and moves westward and northward with time. Ten-year average bimonthly positions of the ice edge and extreme locations derived from the Navy-NOAA JIC sea ice charts are examined for comparison with the 2 years 1979 and 1980. These data show the first open water to occur along the Alaskan coast between May 15 and June 1 [*NOAA*, 1984; *Barry et al.*, 1979]. The clearing of ice in the southern and southwestern Chukchi Sea takes place on the average by July 1. The entire region is then generally ice free by September 15.

In 1979 the weekly Navy-NOAA JIC sea ice charts display

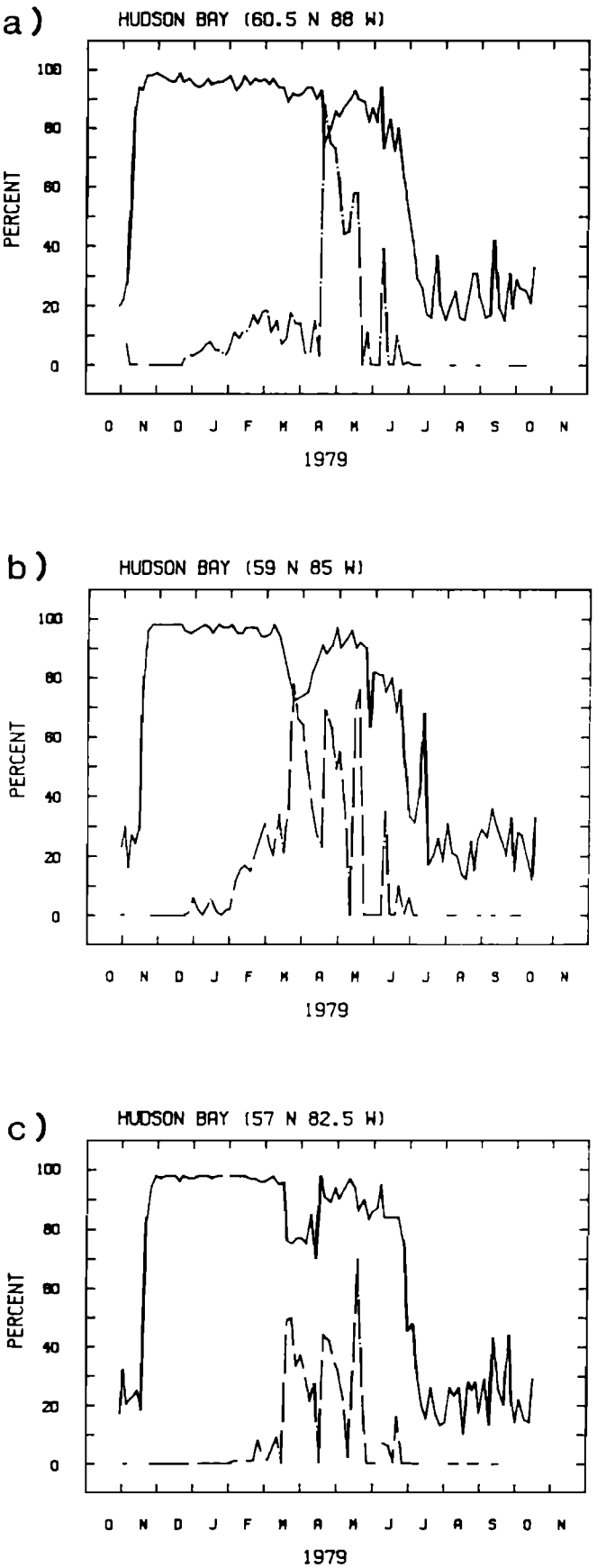

Fig. 9. Time sequence of sea ice concentration (solid line) and multiyear ice fraction (dashed-dotted line) for October 1978 through October 1979 in the (*a*) northern Hudson Bay, (*b*) central Hudson Bay, and (*c*) southeastern Hudson Bay.

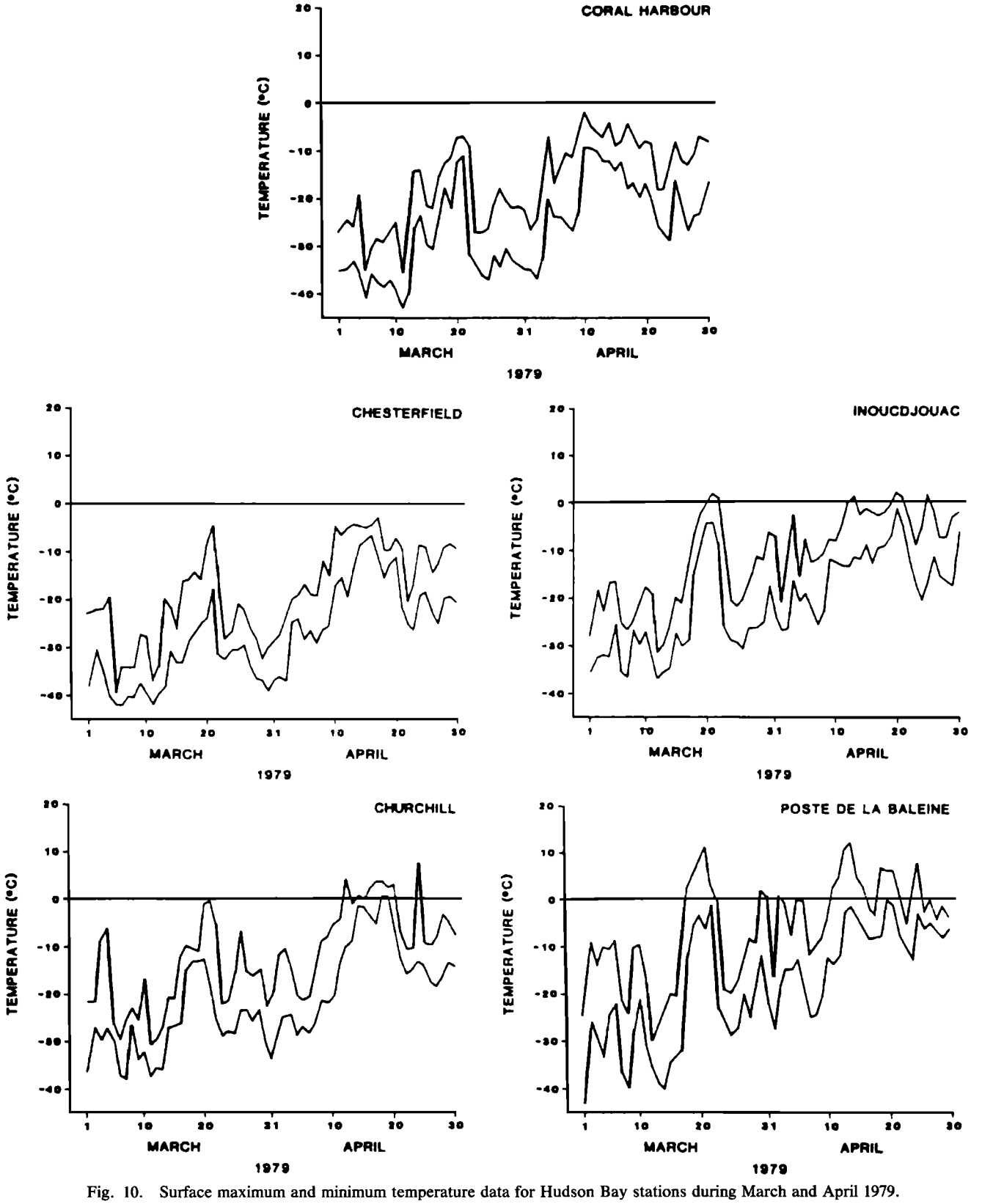

Fig. 10. Surface maximum and minimum temperature data for Hudson Bay stations during March and April 1979.

a much earlier clearing of the ice than normal in the eastern Chukchi Sea. The charts show open water along the Alaskan coast by May 1. By the beginning of June, the area just north of the Bering Strait is also ice free. Ice edge climatology shows this region to be ice covered until the end of June [*NOAA*, 1984]. In summary, the Chukchi Sea clears earlier than normal along the eastern coast and near normal along the western side. This coincides with observations of the melt signatures derived from the 1979 microwave data.

Examination of the 1980 weekly Navy-NOAA JIC ice charts for the region compared with the ice edge climatology shows near normal retreat of the ice throughout the melt

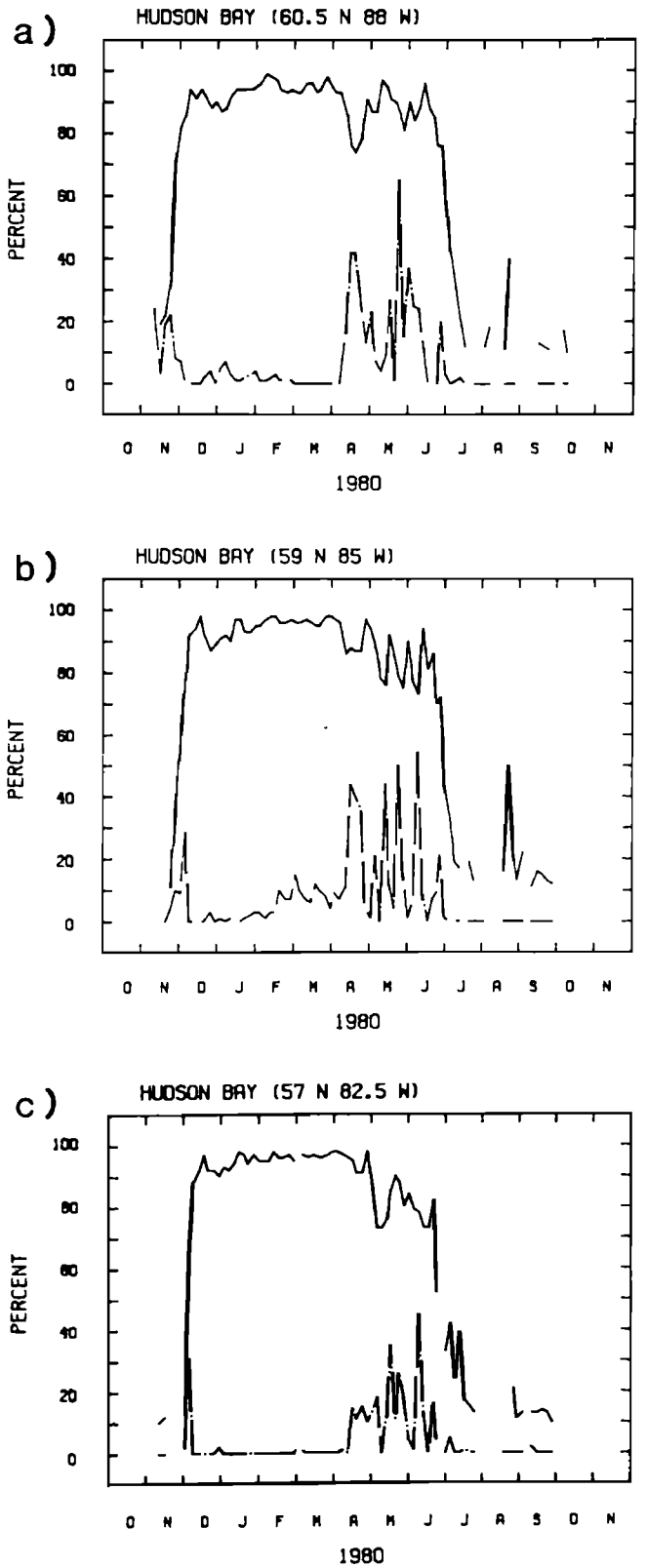

Fig. 11. Time sequence of sea ice concentration (solid line) and multiyear ice fraction (dashed-dotted line) for October 1979 through October 1980 in the (*a*) northern Hudson Bay, (*b*) central Hudson Bay, and (*c*) southeastern Hudson Bay.

period. In addition, the weekly charts display similar sea ice concentrations for both sites from early July through the clearing in August.

The melt signatures for 1980, however, show a different pattern from those for 1979. The time sequences of the multiyear ice fractions show melt signatures occurring at approximately the same time period for both the Alaskan (Figure 4*b*) and Siberian sites (Figure 4*d*) in the Chukchi Sea. The signal appears to be stronger at the Siberian location. In addition, the timing of the event for the Alaskan site occurs 3 to 4 weeks later in 1980 than in 1979. This is in accord with shortwave satellite imagery analysis of melt for the 2 years (D. Robinson, personal communication, 1985). The relatively early nature of the melt and the differences between the two sites may be due to the synoptic weather conditions, but this needs to be investigated further.

East Siberian Sea

Time sequences of sea ice concentrations and multiyear ice fractions for the East Siberian Sea (Figure 1) do not fit the pattern of the other regions investigated. In 1979, no melt signature is observed for the East Siberian Sea (Figure 5*a*). There are two possible explanations. First, during June 1979 the MAP-SS data archive is not complete for this site; however, nearby regions did exhibit a melt signature where data are available during June. The other possible explanation may be related to the surface conditions and the amount of melt taking place. *Lohanick and Grenfell* [1986] found different microwave responses to the amount of snow on the ice surface and the length of time that melt takes place. Unfortunately, snow cover measurements for this time period are not available. The SMMR data also exhibit very little open water in the region as shown by the small reduction of ice concentration (Figure 5*a*). The amount of ice melted by the end of the 1979 summer is also much less than normal [*NOAA*, 1984] which is consistent with a cold summer and the absence of the melt signature during this year.

During the fall the time sequence of the multiyear ice fractions in 1979 indicates that the ice may be draining and becoming second-year ice. This is similar to the situation observed in the northern Laptev Sea (see discussion below).

The multiyear ice melt signature does occur in late May–early June 1980 (Figure 5*b*). This occurrence strengthens the case that one might have observed a similar melt signature during June 1979 if data had been archived. The ice concentration sequence for 1980 shows that the ice clears almost completely by the end of September, about a month later than normal. The ice concentration sequence then displays a rapid freeze-up in October (Figure 5*b*).

Laptev Sea

For the southern Laptev Sea (Figure 1), the multiyear ice melt signatures occur in both years approximately in mid-June, although the signature in 1979 is earlier by one data period (Figure 6). The signal is also greater in 1979 than in 1980.

Even though the timing of these melt signatures is the same, the pattern of ice clearance is different between the 2 years. Analyses of the ice concentrations in Figure 6 show that the ice opens in early August 1980 and persists until late September in 1979. On average, this region should become ice free by September 1 [*NOAA*, 1984].

Data on multiyear ice fractions and ice concentrations were also collected for a second area further to the north, along the edge of the Arctic pack. The time series for both years are represented in Figure 7. The melt signatures occur at approximately the same time for both years. This is

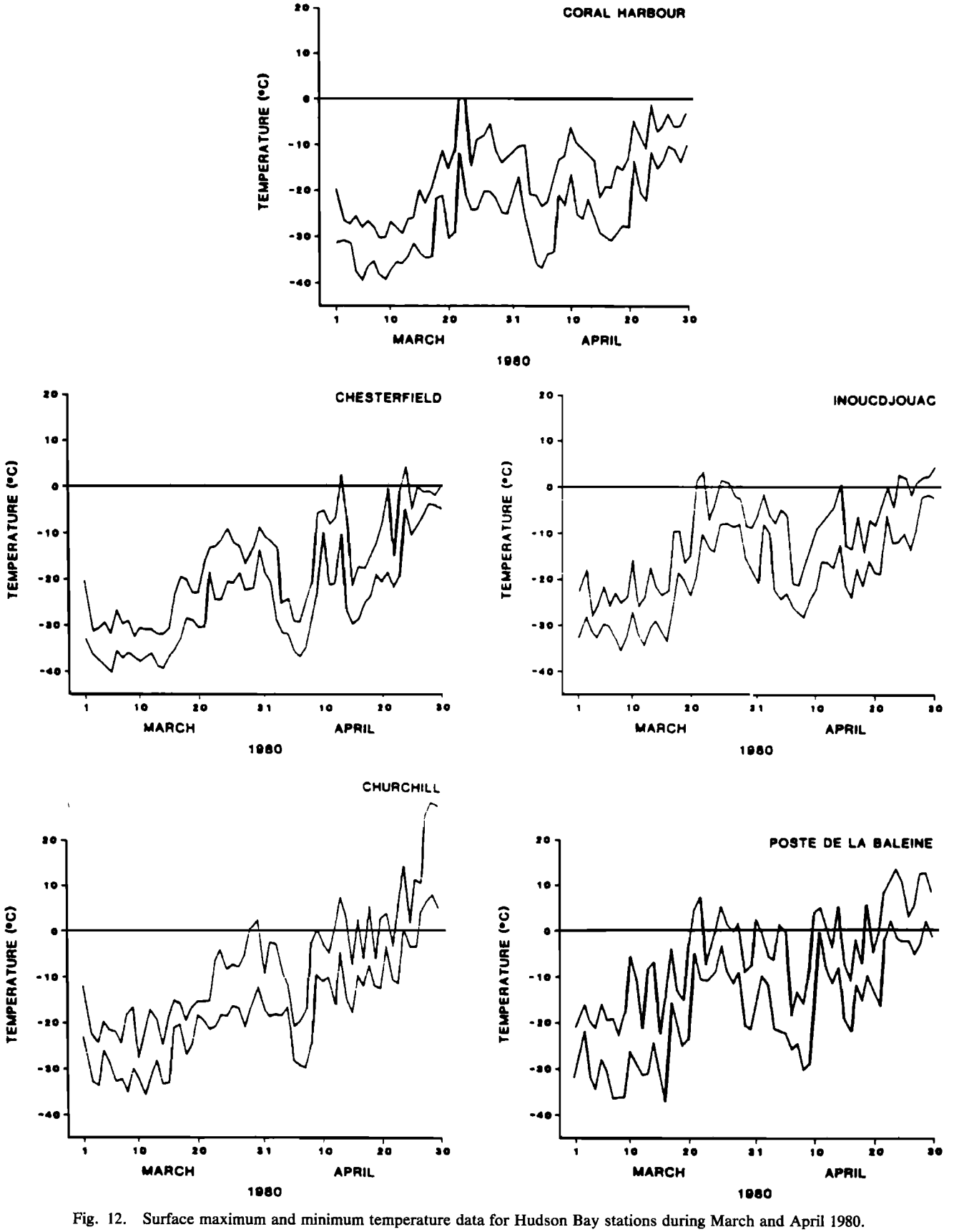

Fig. 12. Surface maximum and minimum temperature data for Hudson Bay stations during March and April 1980.

several weeks later than at the southern location, illustrating a northward movement of melt.

Another feature to observe in the northern case is the progression of the multiyear ice fractions throughout the year (Figure 7). Beginning in late 1978 through early 1979, the multiyear ice fraction decreases from 40% to near zero (Figure 7*a*). This decrease could be caused by the export of ice from this region by the Transpolar Drift Stream [*Colony*

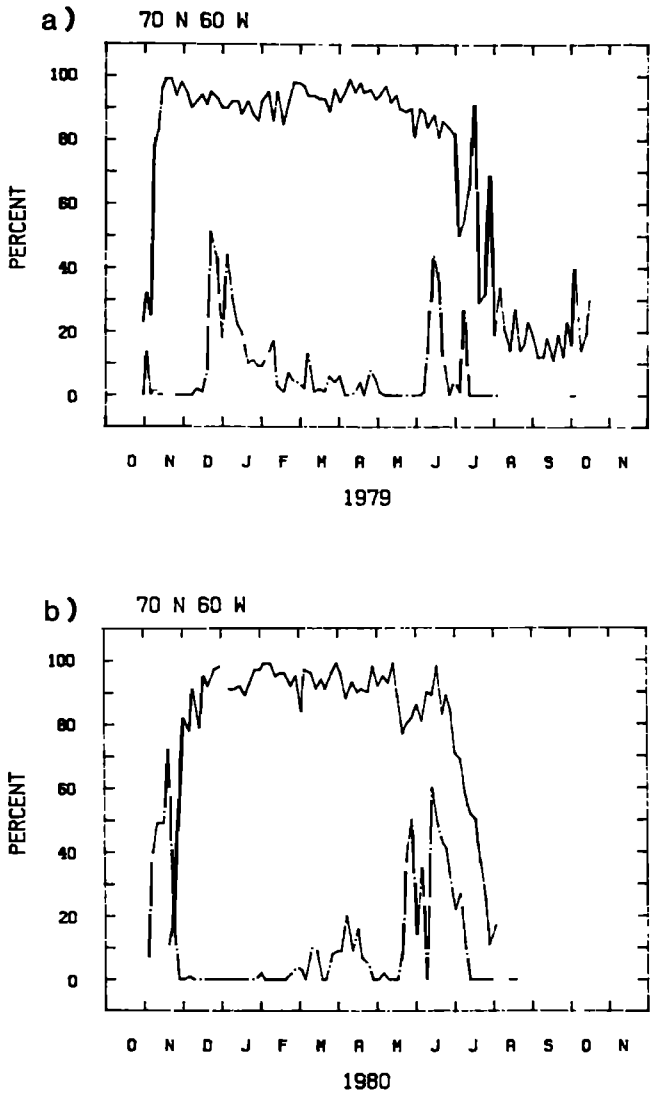

Fig. 13. Time sequence of sea ice concentration (solid line) and multiyear ice fraction (dashed-dotted line) in Baffin Bay for (*a*) October 1978 through October 1979 and (*b*) October 1979 through October 1980.

and Thorndike, 1984]. First-year ice will replace the ice removed from the region, giving the low multiyear ice fractions from mid-March to early June. The total ice concentration remains constant during the period. In early June the melt signature appears and then drops to zero in July. Multiyear ice fractions begin to increase in August probably as a result of the formation of second year ice through the draining of brine. If the multiyear ice fractions are followed through 1980, the same progression is observed (Figure 7*b*). The multiyear ice fractions in the fall of 1980, however, are not as large as those in 1979. This may be a result of more ice melting during the summer of 1980 than 1979 or of the lack of advection into the region.

Hudson Bay

Analysis of the multiyear ice fractions for Hudson Bay also exhibits the melt-freeze signatures for both years, although there are differences in the timing of the events. To display the differences, three locations are chosen for comparison (Figure 8). The first is located in the northern section (centered at 60°N, 88°W), the second is in the southeastern part (57°N, 82.5°W), and the final location is centrally located in between (59°N, 85°W).

In 1979 the southeastern (Figure 9*c*) and middle (Figure 9*b*) sequences show the initial melt to occur in mid-March. The northern location (Figure 9*a*) does not indicate a melt signature until mid-April. The lack of warm air advection into the northern section of the bay may explain the difference between the sites. Examination of the maximum surface air temperatures (Figure 10) during the period for Churchill and Chesterfield on the western shore, Inoucdjouac and Poste de la Baleine on the eastern shore, and Coral Harbour on the northern shore show the distribution of temperature. Above freezing maximum temperatures are reported at the eastern stations during the melt signatures, while the northern and western stations did not record a daily maximum temperature above freezing during the period in question. This would explain the absence of the signature in the northern section.

In April, when another warm episode takes place, melt signatures are observed for all locations. In this case, all meterological stations report maximum temperatures above freezing, with mean daily temperatures between −2.0°C and −4.0°C.

In contrast, there is no observation of a melt signature until April for any of the locations in 1980 (Figure 11). There are several stations that reported above freezing temperatures in March 1980 (Figure 12). However, daily mean temperatures during this period are in the range −6.0°C to −9.0°C. This suggests clear skies with radiational cooling and refreezing of any melt that took place when the temperatures were above freezing. A melt signature does occur in April when maximum temperatures rise above freezing and mean temperatures remain close to the freezing point.

Baffin Bay

The melt signature observations in the Baffin Bay region again show differences between the two study years. In 1979, the occurrence of the melt signature takes place in early June, while in 1980 the occurrence was in late May (Figure 13), a difference of about 3 weeks.

The large pulse in October–November 1980 in Baffin Bay (Figure 13*b*) should be regarded as an error, since the multiyear ice fraction is not calculated for ice concentrations of less than 30%. The signature observed in December 1978 to January 1979, however, could be considered. Examination of the surface air temperatures during the beginning of the period shows above freezing temperatures with the movement of a strong low pressure system through the region, allowing warm air advection to take place. A more complete analysis of this event was not possible within the scope of this project.

5. Summary and Conclusions

This study has determined the variation in the onset of melt at several locations in the Arctic seasonal sea ice zone betwen 1979 and 1980. Detailed analysis of SMMR data for selected locations discloses that the onset of melt in these areas of predominantly first-year ice are observed in the passive microwave data. It is inferred from case studies in the seasonal sea ice zone of Baffin, Chukchi, Kara, Laptev, and East Siberian seas and Hudson Bay that spurious SMMR-derived multiyear ice fractions in these regions dur-

ing the melt season are a result of decreases in brightness temperature caused by melt-freeze cycles on the sea ice surface.

The timing of the melt signature also seems to be related to the ice cover breakup in some regions. For example, in the Chukchi Sea the melt signature appears about 80–90 days before the ice cover clears in both years studied. In the Kara Sea, the same length of time was observed between melt onset and clearing for both years, but the period between onset and clearing was a month longer than it was in the Chukchi Sea case. There are, however, no strong relationships found in the other cases where data were available for both years. Two years of observations are not enough data to draw any solid conclusions concerning relationships between the melt signature and ice breakup; additional years of data need to be analyzed.

A relationship has been established between the calculated multiyear ice fraction and melt in the Arctic seasonal sea ice zone. Currently, work is underway to extend the time series and to expand the analysis to other regions, including the Antarctic where less information is known about the ablation period. The study of these melt events over time can in the future perhaps be used to provide an index of interannual climate variability over ice covered areas.

Acknowledgments. The author would like to thank R. G. Barry and R. G. Crane for their advice and criticism throughout the study. This work was completed as part of the author's dissertation while at the Cooperative Institute for Research in the Environmental Sciences, University of Colorado, Boulder. The research was supported by a National Science Foundation Division of Polar Programs grant (NSF DPP 8217265) and by National Aeronautics and Space Administration grants (NAGW-363, NAG-236, and NAG-1028). The SMMR data were obtained from the National Space Science Data Center.

REFERENCES

Anderson, M. R., R. G. Crane, and R. G. Barry, Characteristics of Arctic Ocean ice determined from SMMR data for 1979: Case studies in the seasonal sea ice zone, *Adv. Space Res.*, 257–261, 1985.

Barry, R. G., R. E. Moritz, and J. C. Rogers, The fast ice regions of the Beaufort and Chukchi Sea coast, Alaska, *Cold Reg. Sci. Technol.*, *1*(2), 129–152, 1979.

Campbell, W. J., P. Gloersen, and H. J. Zwally, Aspects of Arctic sea ice observable by sequential passive microwave observations from the Nimbus-5 satellite, in *Arctic Technology and Policy*, edited by I. Dyer and C. Chryssotomidis, pp. 197–222, Hemisphere, New York, 1984.

Carsey, F. D., Properties for describing and monitoring from space the elements of the seasonal cycle of sea ice, *Ann. Glaciol.*, *5*, 37–42, 1984.

Carsey, F. D., Summer Arctic sea ice character from satellite microwave data, *J. Geophys. Res.*, *90*(C3), 5015–5034, 1985.

Cavalieri, D. J., P. Gloersen, and W. J. Campbell, Determination of sea ice parameters with Nimbus 7 SMMR, *J. Geophys. Res.*, *88*(D4), 5355–5369, 1984.

Chukanin, K. I., Meteorological observations, in *Observational Data in the Scientific-Research Drifting Station of 1950–51* (in Russian), vol. 2, edited by M. M. Somov, pp. 7–217, 1954. (English translation, Arms Service Technical Information Agency, Dayton, Ohio. Available as NTIS AD117139 from Natl. Tech. Inf. Serv., Springfield, Va.)

Colony, R., and A. S. Thorndike, An estimate of the mean field of Arctic sea ice motion, *J. Geophys. Res.*, *89*, 10,623–10,629, 1984.

Comiso, J. C., S. F. Ackley, and A. L. Gordon, Antarctic sea ice microwave signatures and their correlation with in situ ice observations, *J. Geophys. Res.*, *89*(C1), 662–672, 1984.

Gloersen, P., and W. J. Campbell, Observation of variations in the composition of sea ice in the Greenland MIZ during early summer 1983 with the Nimbus-7 SMMR, *Eur. Space Agency Spec. Publ.*, *ESA SP-215*, 373–378, 1984.

Gloersen, P., and L. Hardis, The scanning multichannel microwave radiometer (SMMR) experiment, in *The Nimbus 7 User's Guide*, edited by C. Madrid, pp. 213–243, NASA, Washington, D. C., 1978.

Gloersen, P., et al., A summary of results from the first Nimbus 7 SMMR observations, *J. Geophys. Res.*, *89*(D4) 5335–5344, 1984.

Gow, A. J., Simulated sea ice used for correlating the electrical properties of the ice with its structural and salinity characteristics, paper presented at the 1985 International Geoscience and Remote Sensing Symposium, Inst. of Elec. and Electron. Eng., Amherst, Mass., October 7–9, 1985.

Grenfell, T. C., Multifrequency observations of brightness temperature of artificial new and young sea ice, paper presented at the 1985 International Geoscience and Remote Sensing Symposium, Inst. of Elec. and Electron. Eng., Amherst, Mass., October 7–9, 1985.

Grenfell, T. C., and A. W. Lohanick, Temporal variations of the microwave signatures of sea ice during the late spring and early summer near Mould Bay, NWT, *J. Geophys. Res.*, *90*(C3), 5045–5062, 1985.

Kuznetsov, I. M., and R. A. Timerev, The dependence of ice albedo changes on the ice cover state as determined by airborne observations (in Russian), *Probl. Arkt. Antarkt.*, *40*, 67–74, 1972. (English translation, Israel Program for Scientific Translation, Jerusalem, 1973.)

Lohanick, A. W., and T. C. Grenfell, Variations in brightness temperatures over cold first-year sea ice near Tuktoyaktuk, Northwest Territories, *J. Geophys. Res.*, *91*(C4), 5133–5144, 1986.

Marshunova, M. S., and N. T. Chernigovskiy, *Radiation Regime of the Foreign Arctic* (in Russian), Gidrometeoizdat, Leningrad, 1971. (English translation, *Tech. Translation 72-51034*, 182 pp., Natl. Sci. Found., Washington, D. C., 1978.)

NASA, User's Guide for the Nimbus-7 Scanning Multichannel Microwave Radiometer (SMMR) PARM and MAP Tapes, *Publ. SASC-T-5-5100-0004-016-84*, Washington, D. C., 1984.

National Oceanographic and Atmospheric Administration (NOAA), Oceanographic monthly summary: Eastern-western Arctic sea ice edge climatology, 52 pp., Dept. of Commer., Rockville, Md., 1984.

Stringer, W. T., D. G. Barnett, and R. H. Godin, Handbook for sea ice analysis and forecasting, *Contract. Rep. CR 84-03*, Nav. Environ. Predict. Res. Facil., Monterey, Calif. (Available as NTIS ADA-145286 from Natl. Tech. Inf. Serv., Springfield, Va.)

Yanes, A. V., Melting snow and ice in the central Arctic (in Russian), *Probl. Arkt. Antarkt.*, *11*, 1–13, 1962. (English translation, Arct. Inst. of N. Am., Washington, D. C., 1966.)

M. R. Anderson, Climatology Program, Department of Geography, University of Nebraska, Lincoln, NE 68588.

(Received May 19, 1987;
accepted July 22, 1987.)